Communication

Pb-activated Amine-assisted Photocatalytic Hydrogen Evolution Reaction on Organic-Inorganic Perovskites

Lu Wang, Hai Xiao, Tao Cheng, Youyong Li, and William A. Goddard

Just Accepted

Pb-activated Amine-assisted Photocatalytic Hydrogen Evolution Reaction on Organic-Inorganic Perovskites

Lu Wang[*,†,‡], Hai Xiao[‡], Tao Cheng[‡], Youyong Li[*,†], and William A. Goddard III[*,‡]

[†]Institute of Functional Nano & Soft Materials (FUNSOM), Jiangsu Key Laboratory for Carbon-Based Functional Materials & Devices, Soochow University, Suzhou, Jiangsu 215123, China

[‡]Materials and Process Simulation Center (MSC) and Joint Center for Artificial Photosynthesis (JCAP), California Institute of Technology, Pasadena, California 91125, United States

Supporting Information

ABSTRACT: We report here the reaction mechanism for explicit aqueous solvent quantum mechanics (QM) studies determining the energetics and reaction barriers for the photocatalytic hydrogen evolution reaction (HER) on $CH_3NH_3PbI_3$ surface. We find that both the lead (Pb) atoms and the surface organic molecules play essential roles, leading to a two-step Pb-activated amine-assisted (PbAAA) reaction mechanism involving an intermediate lead hydride state. Both H of H_2 product are extracted from surface organic molecules, while two protons from the solution migrate along water chains via the Grotthuss mechanism to replace the H in organic molecule. We obtain a reaction barrier of 1.08 eV for photochemical generation of H_2 on $CH_3NH_3PbI_3$ compared to 2.61 eV for the dark reaction. We expect this HER mechanism can also apply to the other organic perovskites but the energy barriers and reaction rates may depend on the basicity of electrolyte and intrinsic structures of perovskites.
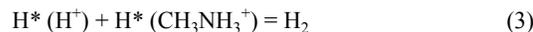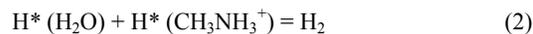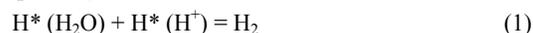
Organic−inorganic hybrid perovskites are being widely applied to solar energy conversion with remarkably strong photovoltaic action and superior solar cell performance.[1,2] The power conversion efficiencies have jumped from 3% to over 20% in just five years. Besides the high solar cell performance, the hybrid perovskites are promising candidates as light-emitting diodes,[3-5] lasers,[6,7] and photodetectors.[8] The high-performance for photovoltaic properties of organic–inorganic hybrid perovskites arises from the low exciton binding energy[9,10] and long carrier lifetime,[11] leading to efficient electron-hole separation and carrier diffusion. These unique properties make the organic-inorganic perovskites promising photocatalytic semiconductors.

Recently, methylammonium lead iodide ($MAPbI_3$) was confirmed as a photocatalyst for H_2 generation in aqueous HI solution.[12] The $MAPbI_3$ powder efficiently splits HI into H_2 and I_3^- under visible light irradiation. In addition, studies on inorganic perovskites suggest them as photocatalysts for carbon dioxide reduction.[13,14] However, there is no reaction mechanism to understand why the perovskites are efficient photocatalysts. Thus, it is important to understand the photocatalytic mechanisms in order to develop improved perovskites materials.

Photocatalytic hydrogen evolution reaction (HER) is an efficient method to convert solar energy to clean energy in the form of H_2. Traditionally, TiO_2 photocatalysts loaded with small amounts of Pt or Rh nanoparticles are utilized as the co-catalysts to generate H_2 by splitting water under the UV light.[15,16] In order to achieve a high conversion efficiency for generating H_2 utilizing visible light, many photocatalytic semiconductors have been developed with suitable band gaps and good separation/migration of photoexcited holes and electrons.[17,18] Here the organic-inorganic perovskites are particularly efficient because of their unique optoelectronic properties. In this communication, we use Quantum Mechanics (QM) in explicit solvent to **derive the reaction mechanism for the photocatalytic HER reaction by the organic−inorganic $MAPbI_3$ perovskite.** We find that, in addition to serving as a photo-absorber for visible light, **the $MAPbI_3$ perovskite serves as a catalyst reductant in the HER reaction with both the lead atoms and the surface organic molecules playing a critical role.**

The computational method are described in Supporting Information. We constructed a 2×2 supercell of the (010) surface of orthorhombic $MAPbI_3$ perovskite in explicit aqueous acidic solution (pH=-0.48) with 3 Molar HI and two potassium atoms added to describe the photoexcited state (the extra two electrons delocalized over the lead atoms). The details of our structural model and the band structures are described and plotted in Fig. S1 of Supporting Information. One can consider four possible reaction pathways for H_2 generation, with the two H atoms forming H_2 derived from H_2O, H_3O^+ or $CH_3NH_3^+$ molecules. These four reaction pathways are:

$$H^* (H_2O) + H^* (H^+) = H_2 \qquad (1)$$

$$H^* (H_2O) + H^* (CH_3NH_3^+) = H_2 \qquad (2)$$

$$H^* (H^+) + H^* (CH_3NH_3^+) = H_2 \qquad (3)$$

$$H^* (CH_3NH_3^+) + H^* (CH_3NH_3^+) = H_2 \qquad (4)$$

First (case a in Fig. 1), we consider the case in which the only role of the $MAPbI_3$ is to absorb visible light with no other involvement in the reaction. In this case, the H atoms of the H_2 derive from H_3O^+ and H_2O in the solution. Here we examined the energetics for one H from H_3O^+ to form H_2 by combining with a nearby H in H_2O. The initial distance between these two H atoms is 3.17 Å and the reaction path involves the H^+ in H_3O^+ moving to the H in H_2O, with the H-H distance decreasing to 1.71 Å in the TS. We calculate an activation barrier of 2.28 eV, which is close

1

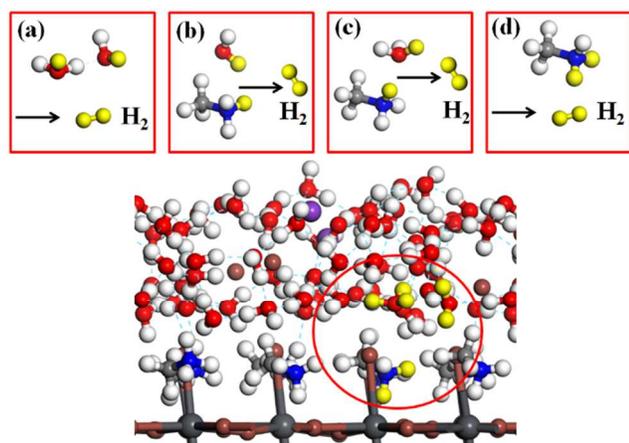to the standard Gibbs free energy of water formation with 2.46 eV.

Fig. 1. Four possible reaction pathways for photocatalytic H_2 generation on the MAPbI$_3$ surface. The upper figure illustrates which H precursors form the H_2 product, while the lower figure shows the structural model and origins of reactants. The two purple balls are the doped potassium atoms.

Second (case b in Fig. 1), we consider that the MAPbI$_3$ could serve as a reactant in addition to absorbing the light. Here we start with one H from an upward -NH$_3$ in MA$^+$, and the other H is from a neighboring H_2O at the interface. The initial distance between these two H is 2.94 Å, which decreases to 2.30 Å in the TS as the H in -NH$_3$ moves toward the H in the H_2O. The reaction barrier for this process is 1.94 eV, which is 0.34 eV lower than the HER reaction between H_2O and H_3O^+, but still quite high.

Third (case c in Fig. 1), we consider that the HER reaction occurs between one H from -NH$_3$ in MA$^+$ and one H from H_3O^+. We choose a downward MA$^+$ interacting with an H_3O^+ at the interface. Here the H in -NH$_3$ starts at an initial distance of 3.79 Å from the H in H_3O^+. Initially, the H in H_3O^+ forms a hydrogen bond with the nearby H_2O molecules in the solution. Along the reaction path the HB to the H_2O breaks and the H moves down to the H of the -NH$_3$ in MA$^+$, while at the same time the orientation of MA$^+$ changes slightly so that the -NH$_3$ orients upward. In the TS, the distance is 1.42 Å between these two H atoms that will form H_2, leading to an energy barrier of 1.34 eV. In this case, there should be an H_3O^+ on the top of a MA$^+$ molecule. However, the concentration of H_3O^+ at the interface is small, reducing the probability for this reaction. The reaction processes and the TS structures for the above three cases can be found in Fig. S2 of Supporting Information.

The remaining possibility is that both H in H_2 derive from surface MA$^+$ cations (case d in Fig. 1). This leads to an intermediate state with one H dissociating from MA$^+$ to form an intermediate state in which this H bonds to the Pb in the lead iodide layer. This extra H atom on the Pb atom breaks the symmetry of lead iodide layer lifting the Pb atom up by 0.4 Å. Prior to binding the H, the Pb atom bonds to four I atoms in the lead iodide layer with bond distances from 3.19 Å to 3.26 Å, but after the formation of Pb-H bond, the Pb atom bonds only with two I atoms at the normal bond distances of 3.13 Å and 3.19Å, while the distances to the other two I atoms in the same layer lie at 3.72 Å and 3.99 Å. Thus,

we can consider that it makes a covalent bond to the H and two half electron ionic bonds to the two I neighbors. Formally the H in Pb-H site can be thought of as H$^-$ with the valence of Pb of +2, so that the excess electron is on the H-Pb site. It is interesting that the intermediate structure has transformed to a semiconductor with the band gap of 2.04 eV, which is shown in Fig. S3 of Supporting Information.

The next step is for another H from an adjacent MA$^+$ molecule to react with the H of the Pb-H to generate H_2 (here for convenience we show both H as coming from the same MA$^+$). This two-step reaction process for HER is shown in Fig. 2. In the first step, the H in the -NH$_3$ starts at 3.09 Å from the nearest Pb atom. Then, as the H migrates from the MA$^+$ to the Pb, the Pb-H distance decreases to 2.17 Å at the TS. At this point, the MA$^+$ becomes a CH$_3$NH$_2$ molecule, with an H from a neighboring H_2O making an HB with the lone pair on the N atom in CH$_3$NH$_2$. This facilitates rotation of the CH$_3$NH$_2$ to form the HB, followed by transfer of the H from H_2O into CH$_3$NH$_2$ molecule to form a new MA$^+$, simultaneous with the H$^+$ from a neighbor H_3O^+ in the solution migrating to form a new H_2O. Thus, there is a Grotthuss chain involving:

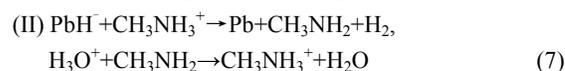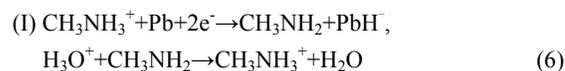$$CH_3NH_2+H_2O+H_3O^+\rightarrow CH_3NH_3^++H_2O+H_2O \qquad (5)$$

The free energy barrier for the proton transferring through water chains by a Grotthuss mechanism is as low as 0.12 eV,[19] which leads to very fast recovery of the surface MA$^+$ cations. Here, the energy barrier for forming the intermediate state is 1.08 eV with consumption of one proton from the solution.

In the second step, we start from the intermediate state of lead hydride with a Pb-H bond distance of 1.97Å with the H pointing toward a surface MA$^+$ molecule at an H-H non-bond distance of 1.35 Å. Due to the H$^-$ at the Pb-H site, the H$^+$ in the MA$^+$ cation moves to PbH$^-$ to generate H_2. Thus, the reaction can be written as: H$^+$+PbH$^-$ = Pb+H$_2$, where the Pb atom loses part of the extra electron to recover the Pb^{2+}. As these two H atoms move to each other to form an H_2 molecule, the H atom on a neighboring H_2O transfers to the CH$_3$NH$_2$ molecule to form a new MA$^+$ cation, simultaneous with the proton from an H_3O^+ transferring to recover this H_2O, another Grotthuss chain as in equation (5).

In this second step reaction, the calculated energy barrier is 0.08 eV with consumption of a second H$^+$, and an exothermicity of 2.30 eV. As shown in Fig. 2, the two H forming H_2 are highlighted by green color for the first H and yellow color for the second H. The diffusion of the proton during the reaction process is highlighted by cyan color. The rate determining step for the H_2 generation is the first step with the energy barrier of 1.08 eV, while the photocatalytic HER reaction releases a total energy of 3.65 eV by consuming two electrons and two protons. This energy barrier is comparable to that of 0.92 eV for photocatalytic HER reaction on TiO$_2$ surface.[20]

Summarizing our calculations, we find the following chemical mechanism for H_2 evolution:

(I) $CH_3NH_3^++Pb+2e^-\rightarrow CH_3NH_2+PbH^-$,

$H_3O^++CH_3NH_2\rightarrow CH_3NH_3^++H_2O \qquad (6)$

(II) $PbH^-+CH_3NH_3^+\rightarrow Pb+CH_3NH_2+H_2$,

$H_3O^++CH_3NH_2\rightarrow CH_3NH_3^++H_2O \qquad (7)$

2

$$(II)\ PbH^- + CH_3NH_3^+ \rightarrow Pb + CH_3NH_2 + H_2$$
$$H_3O^+ + CH_3NH_2 \rightarrow CH_3NH_3^+ + H_2O$$

$$(I)\ CH_3NH_3^+ + Pb + 2e^- \rightarrow CH_3NH_2 + PbH^-$$
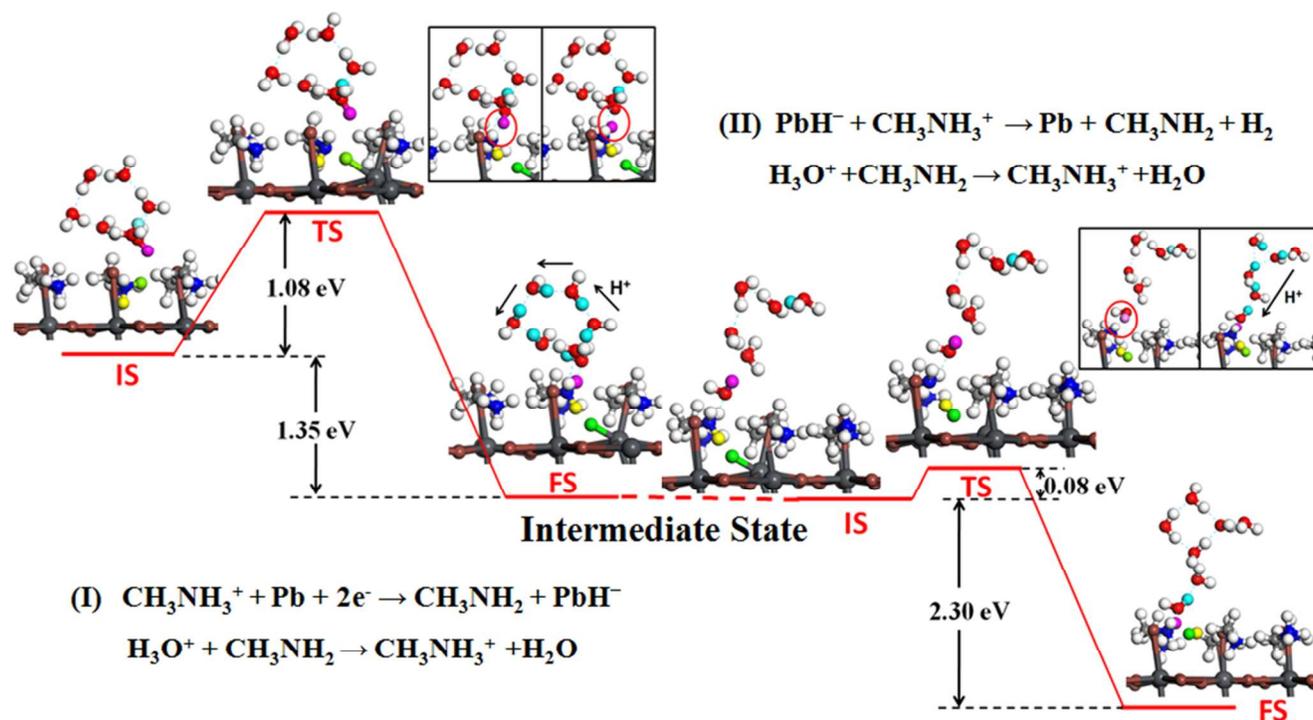$$H_3O^+ + CH_3NH_2 \rightarrow CH_3NH_3^+ + H_2O$$

Fig. 2. Pb-activated amine-assisted (PbAAA) reaction pathway for H_2 generation on MAPbI$_3$ surface in acidic solvent. Most of the water molecules in our system are deleted in this figure in order to see more clearly with the water molecules involved in the diffusion of the protons left. The green and the yellow balls are two H from MA$^+$, and the purple ball is the H in H_2O. The cyan color indicates the proton diffusing along the water chains.

This **Pb-activated amine-assisted (PbAAA) mechanism** involves three important factors that determine the rate of the HER reaction. First, the Pb atom in MAPbI$_3$ plays an important role in promoting the H_2 generation by stabilizing the PbH intermediate state. Second, the flexibility of the surface MA$^+$ molecule allows it to transfer the H to the Pb atom and be re-protonated by the solvent. The third factor is the Grotthuss transfer of H_3O^+ in solution through one or more intermediate H_2O to regenerate the surface MA$^+$ cations. We also calculated the same reaction mechanism for H_2 generation in the dark. We find an energy barrier of 2.61 eV, which is discussed and shown in Fig. S4 of Supporting Information.

Summarizing, we carried out QM calculations in explicit solvent for the photocatalyzed HER reaction on the MAPbI$_3$ surface. This leads to a novel PbAAA kinetic mechanism driven by both Pb atoms and the surface MA$^+$ cations. In the photoexcited state, the excited electrons and holes are separated to promote the Pb and I atoms in the surface lead iodide layer, respectively. We find that the protons of MA$^+$ cation play an essential role in forming H_2 as does the Pb. The reaction involves two steps with an intermediate state forming a Pb-H hydride bond. During the reaction process, two protons in the solution re-protonate the MA$^+$ via a Grotthuss mechanism with rotation of surface MA$^+$ cations to facilitate H_2 generation. We find that, the rate determining first step has an energy barrier of 1.08 eV, with a total energy release of 3.65 eV by consumption of two protons and two electrons. Our results indicate that the chemical nature of the organic perovskites plays a critical role in the photocatalytic HER reaction, serving as a photocatalyst. This suggests designing the perovskites toward their catalysts functionality in addition to their photoexcitation property.

ASSOCIATED CONTENT

Supporting Information

Details of computational method and structural models, discussions on electronic structures for initial and intermediate configurations, the HER reaction paths for case a to c, and the PbAAA mechanism in the dark condition (PDF). The Supporting Information is available free of charge on the ACS Publications website.

AUTHOR INFORMATION

Corresponding Author

*lwang22@suda.edu.cn
*yyli@suda.edu.cn
*wag@wag.caltech.edu

### Notes
The authors declare no competing financial interests.

3

REFERENCES

(1) Xing, G.; Mathews, N.; Sun, S.; Lim, S. S.; Lam, Y. M.; Grätzel, M.; Mhaisalkar, S.; Sum, T. C. *Science* **2013**, *342*, 344.

(2) Burschka, J.; Pellet, N.; Moon, S.-J.; Humphry-Baker, R.; Gao, P.; Nazeeruddin, M. K.; Gratzel, M. *Nature* **2013**, *499*, 316.

(3) Cho, H.; Jeong, S.-H.; Park, M.-H.; Kim, Y.-H.; Wolf, C.; Lee, C.-L.; Heo, J. H.; Sadhanala, A.; Myoung, N.; Yoo, S.; Im, S. H.; Friend, R. H.; Lee, T.-W. *Science* **2015**, *350*, 1222.

(4) Stranks, S. D.; Snaith, H. J. *Nat. Nano.* **2015**, *10*, 391.

(5) Tan, Z.-K.; Moghaddam, R. S.; Lai, M. L.; Docampo, P.; Higler, R.; Deschler, F.; Price, M.; Sadhanala, A.; Pazos, L. M.; Credgington, D.; Hanusch, F.; Bein, T.; Snaith, H. J.; Friend, R. H. *Nat. Nano.* **2014**, *9*, 687.

(6) Xing, G.; Mathews, N.; Lim, S. S.; Yantara, N.; Liu, X.; Sabba, D.; Grätzel, M.; Mhaisalkar, S.; Sum, T. C. *Nat. Mater.* **2014**, *13*, 476.

(7) Zhu, H.; Fu, Y.; Meng, F.; Wu, X.; Gong, Z.; Ding, Q.; Gustafsson, M. V.; Trinh, M. T.; Jin, S.; Zhu, X. Y. *Nat. Mater.* **2015**, *14*, 636.

(8) Ahmadi, M.; Wu, T.; Hu, B. *Adv. Mater.* **2017**, 29, 1605242.

(9) D'Innocenzo, V.; Grancini, G.; Alcocer, M. J. P.; Kandada, A. R. S.; Stranks, S. D.; Lee, M. M.; Lanzani, G.; Snaith, H. J.; Petrozza, A. *Nat. Commun.* **2014**, *5*, 3586.

(10) Miyata, A.; Mitioglu, A.; Plochocka, P.; Portugall, O.; Wang, J. T.-W.; Stranks, S. D.; Snaith, H. J.; Nicholas, R. J. *Nat. Phys.* **2015**, *11*, 582.

(11) Stranks, S. D.; Eperon, G. E.; Grancini, G.; Menelaou, C.; Alcocer, M. J. P.; Leijtens, T.; Herz, L. M.; Petrozza, A.; Snaith, H. J. *Science* **2013**, *342*, 341.

(12) Park, S.; Chang, W. J.; Lee, C. W.; Park, S.; Ahn, H.-Y.; Nam, K. T. *Nat. Energy* **2016**, *2*, 16185.

(13) Hou, J.; Cao, S.; Wu, Y.; Gao, Z.; Liang, F.; Sun, Y.; Lin, Z.; Sun, L. *Chem.-Eur. J.* **2017**, *23*, 9481.

(14) Xu, Y.-F.; Yang, M.-Z.; Chen, B.-X.; Wang, X.-D.; Chen, H.-Y.; Kuang, D.-B.; Su, C.-Y. *J. Am. Chem. Soc.* **2017**, *139*, 5660.

(15) Fujishima, A.; Honda, K. *Nature* **1972**, *238*, 37.

(16) Schrauzer, G. N.; Guth, T. D. *J. Am. Chem. Soc.* **1977**, *99*, 7189.

(17) Chen, X.; Shen, S.; Guo, L.; Mao, S. S. *Chem. Rev.* **2010**, *110*, 6503.

(18) Hisatomi, T.; Kubota, J.; Domen, K. *Chem. Soc. Rev.* **2014**, *43*, 7520.

(19) Cheng, T.; Goddard, W. A.; An, Q.; Xiao, H.; Merinov, B.; Morozov, S. *Phys. Chem. Chem. Phys.* **2017**, *19*, 2666.

(20) Lucking, M.; Sun, Y.-Y.; West, D.; Zhang, S. *Phys. Chem. Chem. Phys.* **2015**, *17*, 16779.

4
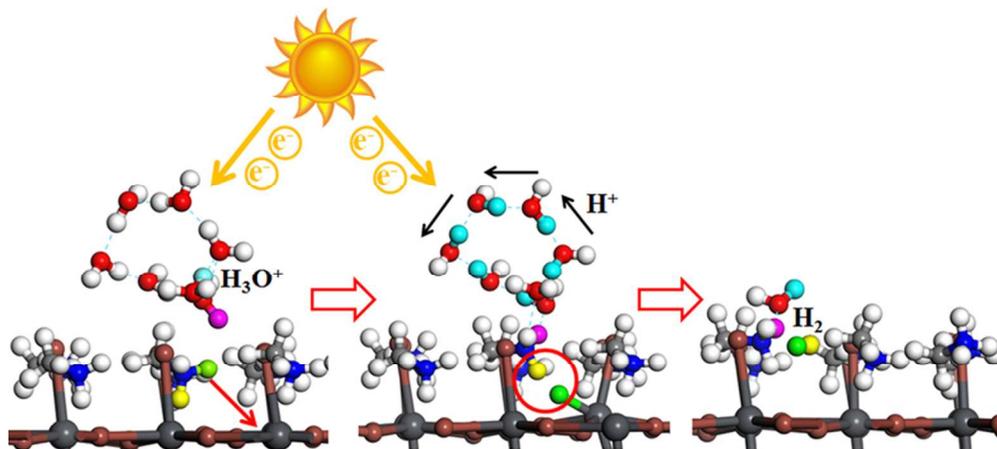
Organic-Inorganic perovskite converts visible light plus protons to PbH hydride and then to H_2.

37x16mm (600 x 600 DPI)